Reconfigurable Antennas Based on Plasma Reflectors and Cylindrical Slotted Waveguide

Fatemeh Sadeghikia, Ali Karami Horestani, Mohamed Himdi

Chapter

Reconfigurable Antennas Based on Plasma Reflectors and Cylindrical Slotted Waveguide

Fatemeh Sadeghikia, Ali Karami Horestani and Mohamed Himdi

Abstract

In this chapter, we focus on the application of plasma structures to realize reconfigurable antennas. Several approaches are presented to dynamically control the beamwidth and radiation gain of circularly polarized helical antennas based on plasma reflectors. Ideas and design principles were discussed and confirmed by full-wave simulations and measurements of realized prototypes. It is shown that plasma reflectors can be effectively used to design reconfigurable helicone antennas with controllable gain and beamwidth. The chapter also presents a reconfigurable slotted antenna using a plasma tube inside the metallic waveguide. It is shown that the radiation pattern of the antenna can be readily reconfigured by changing the state of the plasma column. In short, it is shown that in contrast to conventional methods based on electronic or mechanical devices, reconfigurable antennas based on plasma media benefit from simple and relatively low-cost structures as well as high performance.

Keywords: plasma technology, reconfigurable antenna, beam steering, beamwidth control, helicone antenna

1. Introduction

During past decades, potential applications of reconfigurable antennas in single-input single-output (SISO) and multiple-input multiple-output MIMO communication systems have been widely investigated [1–32]. In both cases, the principal objective is to reduce the complexity of communication systems by obtaining diverse radiation patterns and operating frequencies. For example, beam-steerable antennas can provide multiple functionalities, thus, mitigating the complexity and overall cost of communication systems.

Regarding applications in reconfigurable antennas, partially ionized plasma elements have the potential to be used either as the main radiator of the antenna as a reflector, a parasitic director element, or even as a dielectric to improve the performance of conventional antennas. Various realizations of antennas with reconfigurable radiation characteristics and/or tunable resonance frequencies based on plasma radiating element (s) have been reported in [1, 10–32]. However, due to the finite

conductivity of the plasma elements, these antennas generally suffer from low efficiency [12, 33]. This problem may be worse for small plasma antennas on which there are high current densities. It can be seen, however, that since the current density on the reflecting and parasitic elements of an antenna is much smaller than on the main radiator of the antenna, plasma conductors may be good surrogates for metallic reflector structures. The main advantage of using plasma reflectors rather than metallic ones is that plasma reflectors can be switched on or off to toggle between original and modified radiation patterns. This feature is demanded in many applications. For instance, when radiation patterns with an adjustable beamwidth or main direction are needed. In brief, a combination of plasma elements as reflectors and metallic element (s) as the main radiator results in highly efficient reconfigurable antennas. In view of these advantages, this chapter focuses on applications of plasma media as reflectors (rather than the main radiator) for the realization of reconfigurable antennas.

The chapter is organized as follows. In Section 2, the characteristics of the plasma media and the electromagnetic waves propagating in such media are briefly reviewed. In Section 3, the benefits of the application of the plasma reflectors along with conventional metallic antennas are described and two different prototypes, namely, a plasma-cupped-ground helical antenna and a plasma helicone antenna are introduced. For each prototype, the basic structure and the implementation technique are discussed and their radiation characteristics are presented. The study will be concluded in Section 4.

2. Theory of plasma

In order to investigate the effect of plasma media on the radiation characteristics of antennas, some basic properties of the plasma are first presented in this section.

The complex permittivity up of an isotropic plasma at low pressure can be modeled as follows:

$$\frac{\varepsilon_p}{\varepsilon_0} = \left(1 - \frac{\omega_p^2}{\omega^2 + \upsilon^2}\right) - j\left(\frac{\omega_p^2 \upsilon}{\omega(\omega^2 + \upsilon^2)}\right) \tag{1}$$

Based on this relation, the plasma is a dispersive medium with permittivity εp, which is a function of the operating angular frequency ω (rad/s). The permittivity of the plasma is also a function of the electron-neutral collision frequency υ in Hz, and the plasma angular frequency ω_p (rad/s), which is defined as follows [13, 14]:

$$\omega_p = \left(\frac{ne^2}{m\varepsilon_0}\right)^{\frac{1}{2}} \tag{2}$$

where n is the electron density (m^{-3}), e is the electron charge, and m is the electron mass (kg). The electrical conductivity σ is given by [14]:

$$\sigma = \left(\frac{\varepsilon_0 \upsilon \omega_p^2}{\upsilon^2 + \omega^2}\right) - j\left(\frac{\varepsilon_0 \omega \omega_p^2}{\upsilon^2 + \omega^2}\right) \tag{3}$$

This relation thus indicates that the electrical conductivity of the plasma can be controlled at a given operating frequency by varying either the plasma frequency or

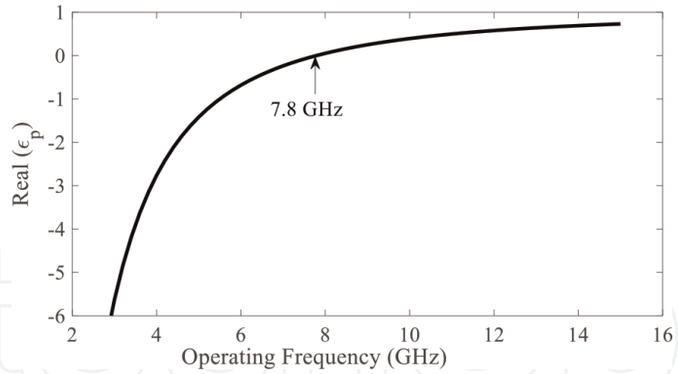

Figure 1.
Variations of the permittivity of the plasma medium versus the frequency for the plasma frequency of 7.8 GHz and the collision frequency of fp/3.

the collision frequency. The loss factor tanδ of the plasma medium can be derived from the ratio of the imaginary part to the real part of the plasma dielectric constant as follows:

$$\tan\delta = \frac{\varepsilon_i}{\varepsilon_r} = \frac{-\left(\frac{\omega_p^2 \nu}{\omega(\omega^2+\nu^2)}\right)}{\left(1-\frac{\omega_p^2}{\omega^2+\nu^2}\right)} = -\frac{\nu\omega_p^2}{\omega\left(\omega^2+\nu^2-\omega_p^2\right)} \tag{4}$$

Based on this relation, plasma loss is a function of plasma parameters and operating frequency.

From Eq. (1), the plasma medium acts as a dielectric with a positive permittivity for incident EM waves with frequencies higher than the plasma frequency, thereby allowing the propagation of the incident wave through the plasma medium. I understand this. In contrast, at frequencies less than the plasma frequency, the plasma shows a negative permittivity, thus prohibiting the propagation of the EM wave. At frequencies much lower than the plasma frequency, the plasma medium can be used as a conductor, but it is not a very good conductor. For instance, in **Figure 1**, variations of the real part of the plasma permittivity versus the operating frequency, for a medium with the plasma frequency f_p = 7.8 GHz and the collision frequency $\upsilon = f_p/3$ are shown. It is observed that at the frequencies below the plasma frequency, the plasma permittivity is negative, thus the plasma reflects the incident wave. However, at frequencies greater than 7.8 GHz, the plasma permittivity varies from 0 to 1, thus the plasma acts as a dielectric. It is also important to note that, since the plasma angular frequency ω_p can be tuned by adjusting some of the characteristics of the plasma, such as its density, the frequency band in which the plasma behaves as a dielectric or a conductor is adjustable.

3. Application of plasma reflectors in the antenna structures

Application of the plasma reflectors along with conventional metallic antennas may provide benefits including steering capability and/or beamwidth control. In general, a variety of methods are available to control the radiation pattern of directional antennas. However, almost all of these methods employ a kind of switching mechanism including electrical, optical, or mechanical switches which require

complex and costly feed circuitries [5–7]. Altering the substrate characteristics by using materials such as liquid crystals, ferrites, or plasmas is an almost new alternative method for steering the radiation pattern of the antennas. The unique properties of plasma as the fourth state of the matter have opened a new perspective for the realization of antennas with a reconfigurable radiation pattern or a tunable operating frequency. Therefore, plasma-based reconfigurable/tunable antennas can be considered as cost-efficient and efficient alternatives for currently in-use methods [2, 4, 8, 9]. As shown in the previous section, the plasma medium can be used as a conductor at frequencies much lower than the plasma frequency. An important advantage of plasma-conducting elements compared to metallic ones is that they can be switched on and off and their length can be adjusted electrically. Authors [2, 4, 8, 9, 34, 35] investigated theoretical aspects and different configurations of metal antennas with plasma reflectors for manipulating antenna radiation patterns.

Although various techniques have been introduced to control the beamwidth of antennas, including the use of liquid metal reflectors [36], conformal selective surfaces [37], and varactor switches, antenna beam steering and beamwidth control There has been little research done on the simultaneous execution of Single antenna architecture [38–39]. However, in these studies, antenna beam steering and beamwidth control increased the cost of hardware and software complexity. It has been shown by authors [40] that a reconfigurable antenna based on plasma reflectors not only may be able to steer the radiation pattern in 3-D space but also can be used for the dynamic control of the antenna beamwidth. Based on these advantages and recent trends in scientific reporting, we believe it is likely that the next decade will see a significant increase in research on plasma-based communication components, including reconfigurable antennas. Therefore, in this section, we present here two prototypes of reconfigurable antennas based on plasma reflectors and analyze their radiation properties. In both cases, a conventional axial-mode helical antenna is used as the primary radiator, and a plasma reflector is used to steer the beam or change the beamwidth of the antenna.

3.1 Plasma-cupped-ground helical antenna

The first part of this section presents the structure of a conventional dish ground axial mode helical antenna and compares its radiation pattern with that of an identical planar ground antenna. In the following, we consider an axial mode helical antenna with a plane ground as the reference antenna. In addition, we study the effect of the height of the dish bottom on the radiation properties of the antenna, including the gain and half-width (HPBW) of the antenna. Part 2 investigates the feasibility of beamwidth control based on plasma elements by replacing the metal dish ground of the helical antenna with a plasma dish ground and numerically comparing the characteristics of the two antennas. Then, the final part of this section describes the realization and experimental verification of the proposed antenna.

3.1.1 Structure and dimensions of dish bottom helical antenna

Various methods have been proposed in the literature to improve the radiation properties of helical antennas. Authors [41–44] considered modifying the ground plane of the antenna to form a cup-shaped ground reflector. Despite its simplicity, this method is very effective in improving the beamwidth and radiation gain of helical antennas. **Figure 2** shows the shape of a conventional dish-bottom helical antenna. The antenna consists of a helical antenna operating in on-axis mode and a dished

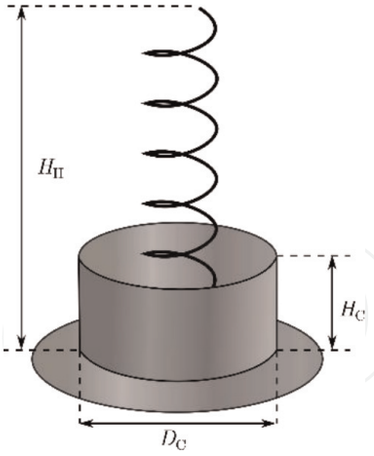

Figure 2.
The structure of a typical cupped ground helical antenna.

metal reflector. It can be shown that the cup-shaped reflector with the height of H_C, and the diameter D_C can improve the radiation gain and the HPBW of the antenna. Note that the achieved gain depends on the dimensions of the cup, including its height and radius. For demonstration, the effect of the height H_C of the cup on the radiation gain and HPBW of the helical antenna is shown in **Figure 3**. The antenna operates at the center frequency of 927 MHz and has an antenna diameter of D_c = 330 mm ($\sim \lambda$). Simulation results are shown for three different numbers with turns N = 6.5, 10, and 13. In this study, the diameter of the helix is D_H = 116 mm, the pitch angle α = 13.6°, and the helix height H_H = 550 mm. The designed helical antenna with a planar ground conductor with a radius D_g = 480 mm demonstrates a simulated radiation gain of 12.7 dBi and the HPBW of 37.5° at the center frequency. The full-wave simulated radiation gain and HPBW of the antennas versus the height of the cupped ground (normalized to the helix height, i.e., H_C/H_H) show that increasing the height H_C of the cupped ground up to around H_C/H_H = 0.07 when N = 6.5 in this study, enhances the gain of the antenna up to 0.5 dB. However, further increasing the H_C, decreases the gain and consequently, increases the HPBW of the antenna. For instance, when H_C/H_H = 0.29 (i.e., H_C = 160 mm for N = 6.5), the radiation gain of the antenna with respect to the reference helical antenna decreases around 0.4 dB, while the HPBW increases around 7.5°. **Figure 4** compares the simulated radiation gain of the reference antenna with that of the cupped ground helical antenna when H_C = 160 mm for N = 6.5.

It can be concluded here that HPBW and the maximum radiation gain of the helical antenna can be adjusted by the height of the cupped ground. The results also show the potential application of the tunable length plasma cup for controlling the radiation

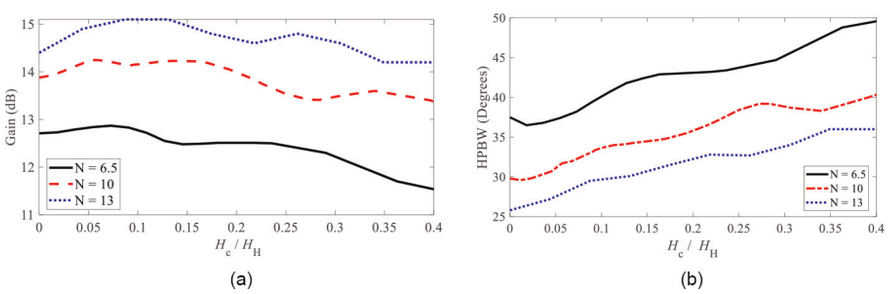

Figure 3.
Simulated Gain and HPBW of the cupped ground helical antenna versus H_C/H_H considering the constant height of the helix (H_H).

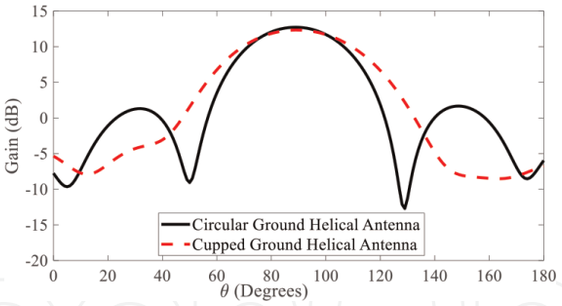

Figure 4.
A comparison between the simulated radiation gain of a conventional helical antenna with a planar ground and the cupped ground helical antenna with H_C = 160 mm.

gain and beamwidth of helical antennas. Thus, in the next section, first, the metallic cup of the helix antenna is replaced with a plasma cup with H_C = 160 mm, and the effects of different configurations of the plasma reflector on the performance of the plasma-based and metallic antenna will be compared.

3.1.2 Plasma reflectors as the cupped ground for a helical antenna

It is worth reminding that if the plasma frequency is sufficiently larger than the operating frequency, the plasma medium demonstrates a relatively high conductivity. Therefore, if the metallic cup in the antenna is replaced with a plasma cup, the efficiency of the antenna with a cup-shaped plasma reflector depends on the plasma frequency. To further investigate this effect, two different plasma frequencies f_{p1} = 3 GHz and f_{p2} = 30 GHz for the plasma-cupped ground in a helical antenna with identical dimensions as the antenna presented in the previous section are studied. In **Figure 5**, the radiation gain of the antenna for the two plasma frequencies f_{p1} = 3 GHz and f_{p2} = 30 GHz is plotted. The results are also compared to the radiation gain of the helical antenna with a metallic planar ground as well as the gain of the antenna with metallic-cupped ground. As shown in this figure, the gain of the first plasma-cupped antenna shows no improvement with respect to the gain of the helical antenna with a planar ground. This is because the conductivity of the plasma cup with the plasma frequency f_{p1} = 3 GHz is not adequate to act as a good reflector. In contrast, for the higher plasma frequency of f_{p2} = 30 GHz, the plasma behaves nearly the same as a metallic cup, leading to improved gain. In short, the simulation results show that the metallic reflector can be replaced with the plasma reflector if the plasma frequency for the plasma reflector is properly chosen.

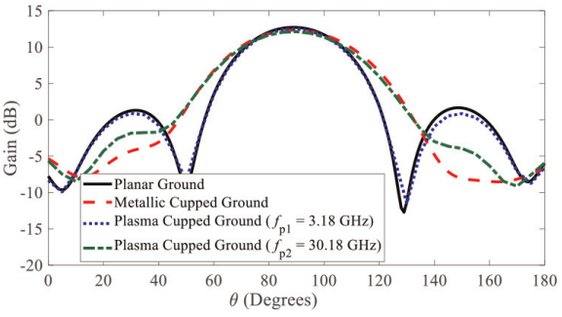

Figure 5.
Simulated radiation gain of a cup-helix antenna with different cup materials compared to a conventional flat-bottom helix antenna.

It is worth noting that achieving a uniform plasma surface is demanding and expensive. However, an array of plasma columns dense enough to form the cup-shaped bottom 10 can be used. For this purpose, taking into account the various types of commercially available plasma tubes. In this study, a compact U-shaped fluorescent lamp (CFL) is used to implement the plasma reflector. An array of 25 CFLs arranged in a circle around the helix is used, as shown in **Figure 6a**. As shown in **Figure 6b**, the actual size of commercial type CFL is considered in this investigation for the geometric scales of the reflectors. In this study, the height of each CFL from the ground plane is 160 mm while its diameter is 14.7 mm leaving a 1.6 mm space gap between the columns of the CFL.

Using this configuration, variations of the number and arrangement of the activated CFL reflectors shape the beam profile of the radiated wave. For the beamwidth adjustment, three configurations are studied in this investigation. The first configuration is called the all-off state, with all CFLs off (), the second configuration with 12 alternate CFLs; on (), and the final configuration with the all-on state. All elements are known to be on ()

For simulation purposes, the plasma frequency and collision frequency of the CFL are assumed to be $\omega = 14 \times 10$ rad/s and $\nu = 400$ MHz, respectively. Also, his commercially available CFL tube components are modeled as Pyrex with a dielectric constant of 4.82. and 0.5mm thick. Additionally, inactive CFL tubes are only simulated as empty U-shaped Pyrex tubes. For simulation purposes, a loss factor $\tan\delta = 0.069$ at the operating frequency f = 927 MHz is considered. As already mentioned, plasma medium losses are higher than conventional conductors. However, since the plasma element is used as a reflector rather than the antenna's main radiator, the performance of the antenna is not degraded. However, some of the physical parameters of the plasma, such as pressure, can be used to further reduce the effects of plasma leakage [45].

Figure 7 shows the simulated antenna radiation gain for the three configurations. As shown in this figure, a relatively narrow radiated beam, which is around 37°, exactly the same as the radiated beam of the helical antenna with no reflector, belongs to the All-OFF state, while a wider beam and a lower gain are achieved by the 12 alternatively turned-on. Increasing the number of activated CFLs makes the beam

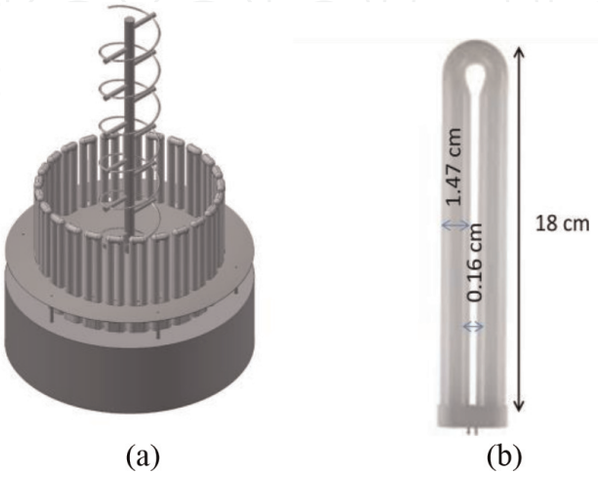

Figure 6.
(a). Geometry configuration of a plasma-cupped-ground helical antenna based on the CFL reflectors. (b). Geometry of the reflective CFL elements.

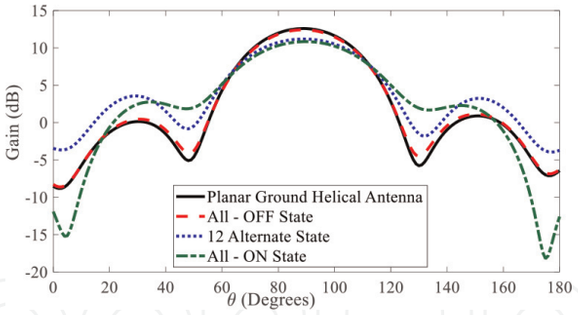

Figure 7.
Simulated radiation gain of the cupped ground helical antenna using plasma reflectors.

even wider and it covers a wider space angle. Therefore, the widest beam, which is around 50.3°, is observed at the direction of the end-fire when all the CFLs are activated and as expected, the gain adversely decreases from 12.5 dBi for the All-OFF state to 9.21 dBi for the All-ON state. In short, as shown in **Figure 8**, due to the diffraction of electromagnetic waves, when a higher number of plasma reflectors is activated, the radiation gain decreases.

Another desirable characteristic of the plasma-cupped-ground helical antenna is that by unsymmetrical activation of a group of neighboring CFLs the main radiation lobe of the antenna can be steered. The radiation patterns of the antenna for two configurations, including the case in which half of the adjacent reflectors (i.e., a half-cylinder) on the right side are turned ON and the CFLs in the left half cylinder are turned OFF, and also the case with its complementary configuration, in which the CFLs in the right half cylinder are turned OFF and those in the left half cylinder are turned ON, are compared and the results are shown in **Figure 9**. The figure clearly shows that the beam of the antenna can be steered by ±6° electrically by this method. Note that the beam steering in a three-dimensional space around the end-fire direction of the antenna can be performed by activating a half cylinder of CFL array, while the height and radius of the cup change the scanning angle. Although the dimensions of the commercially available plasma tubes used in this study enforce the height of the plasma cup, in practical applications customized plasma tubes can be used to bypass the barrier of steering angle.

In short, through full-wave electromagnetic simulations it is demonstrated that, using a dense array of plasma CFLs instead of a metallic cup, the radiated beamwidth of a helical antenna can be electrically controlled, while its direction has the potential to be steered in the space.

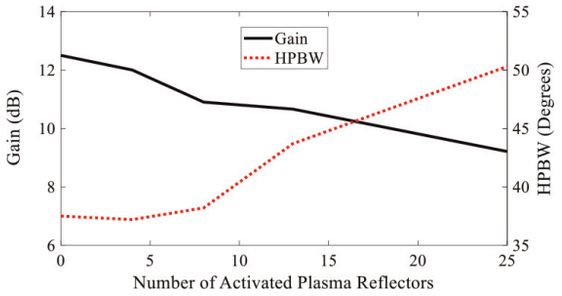

Figure 8.
Variations of the simulated radiation gain and HPBW of the cupped ground helical antenna versus the number of symmetrically excited plasma reflectors.

DOI: http://dx.doi.org/10.5772/intechopen.108017

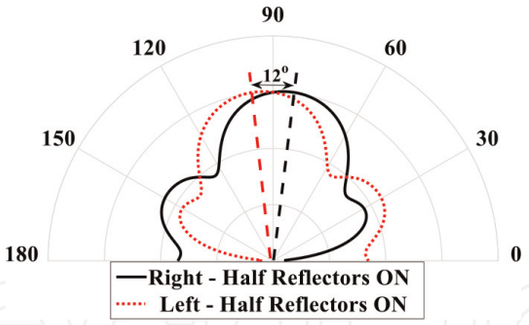

Figure 9.
Simulation results of the steered radiation pattern of the helical antenna using activation of the half number of CFLs.

3.1.3 Realization of the antenna and measurement results

The details of the realization and experimental validation of the plasma-cupped-ground helical antenna are devoted in this section. To this end, a prototype of the antenna is implemented and a comparison between simulated and measured results is presented.

By assembling the main body of the helical antenna and the plasma CFLs on a circular ground structure, as shown in **Figure 10a** and **b**, a prototype of the proposed antenna is realized. In this structure, each CFL is supplied by an electrical ballast which is connected to a relay. The states of each relay are controlled independently by a microcontroller board and as a result, every single CFL can be switched ON or OFF independently to control the radiation beamwidth or to steer the radiated beam toward the desired direction. The block diagram of the details of the reflector structure, including the CFLs and controlling electronic devices, is shown in **Figure 10c**.

Measurements are performed in an anechoic chamber with peak gain accuracy better than 0.5 dBi within the operating frequency range of the antenna. A comparison of simulated and measured antenna radiation gains for various plasma reflector configurations is shown in **Figure 11**. The measured gain and HPBW in the fully off state are 12.2 dBi and 42o, respectively, slightly wider than the simulated HPBW in this state. The measured gains for the all-element active and 13 alternately active configurations are 9.18 and 10.07 dBi, respectively, and the HPBW are 51.5o and 42.4o, respectively. In short, the good agreement between the simulation and

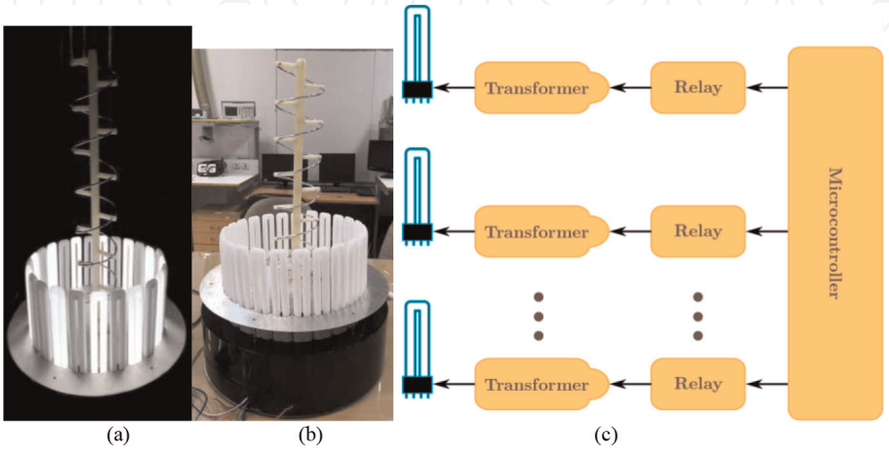

Figure 10.
(a), (b) Fabricated antenna, (c) Block diagram of the details of the structure of the showing antenna.

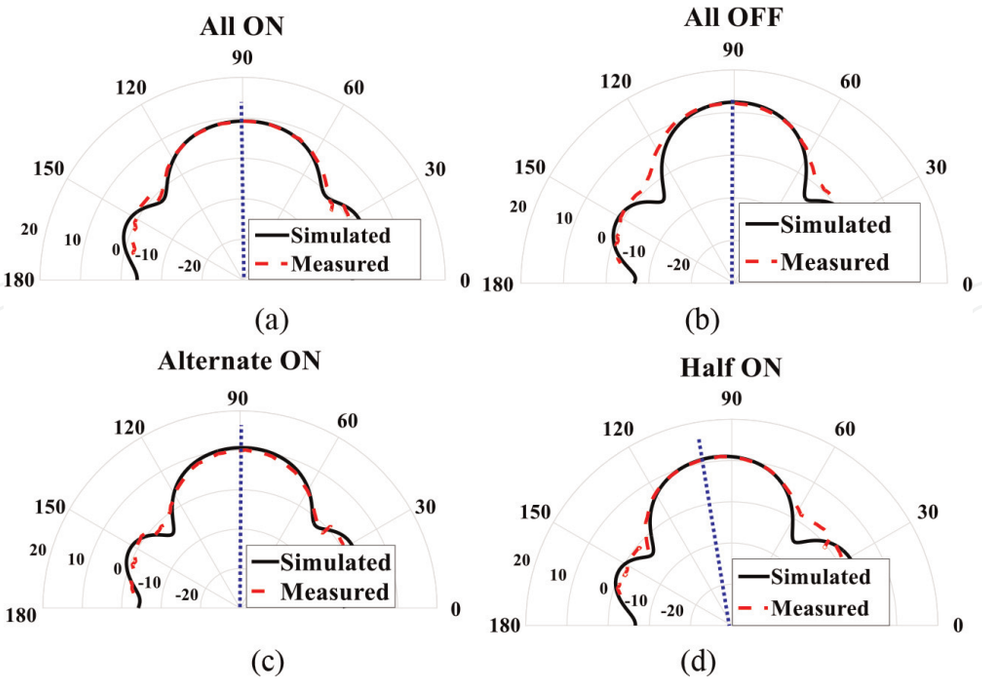

Figure 11.
Comparison of simulated and measured radiation gains of a plasma dish antenna at a frequency of 927 MHz for various configurations: (a) all CFLs active; (b) all CFLs are deactivated; (c) CFL is activated alternately; and (d) half of the adjacent CFL becomes active.

measurement results of the configuration confirms the simulation results related to the proposed method of electronic control of the antenna beamwidth. In total, 25 CFLs (odd number of CFLs) are used in this study to fully cover the cup bottom situation. Therefore, this mode is not a completely symmetrical configuration because alternating CFL activations leave two adjacent CFLs both activated (or deactivated). Therefore, some asymmetry in the radiation gain is expected. The time required to change the width or direction of the radiation beam depends only on the plasma decay time. This is about a few microseconds.

To experimentally verify the beam-steering capability of the proposed antenna, only 12 CFLs on one side of the bottom of the plasma cup are turned on and the remaining CFLs are turned off. The measured gain, in this case, is about 11.07 dBi at 96o, which matches very well with the simulated gain of 11.10 dBi, as shown in **Figure 11d**. In summary, the proposed technique for steering the beam and controlling the beamwidth using plasma reflectors is validated both numerically and experimentally.

3.1.4 Application of a half-cup plasma reflector for beam steering

An investigation on the effects of the dimensions of a half-cup plasma reflector, including its height HC and diameter DC, on the radiation characteristics of the helical antenna to control its steering angle will be presented in this section [46].

4. The effect of the diameter of the half-cup plasma reflector

To investigate the effect of the diameter of the half-cup D_C on the radiation characteristics of the antenna, a parametric study is conducted in this section. In this

DOI: http://dx.doi.org/10.5772/intechopen.108017

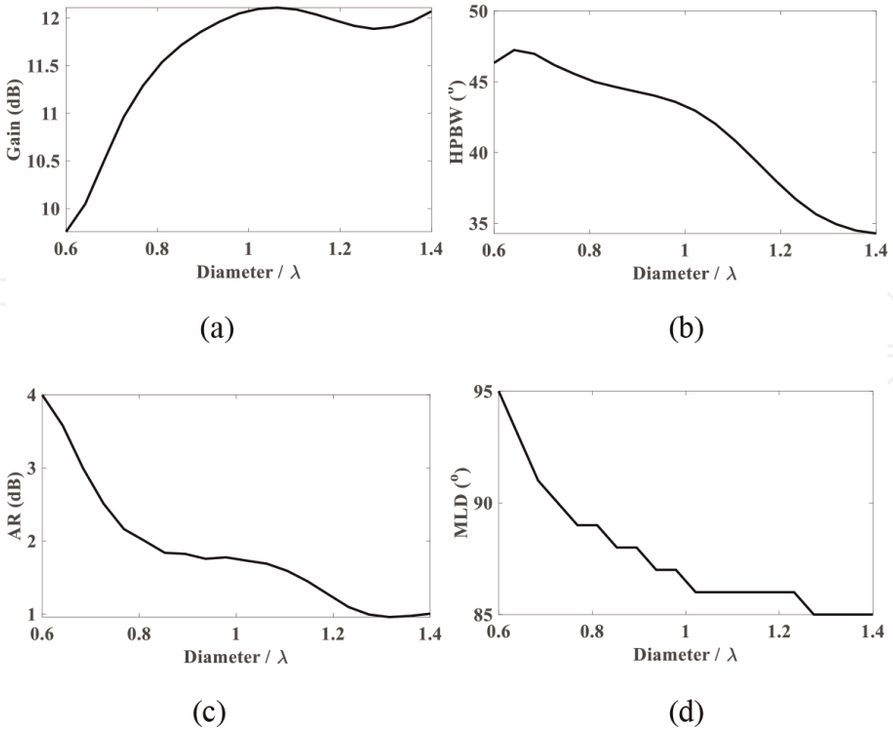

Figure 12.
Radiation characteristics of the plasma half-cupped-helical antenna with a diameter of the cup at H_C = 0.5 λ: (a) gain, (b) half-power beamwidth (HPBW), (c) axial ratio (AR), and (d) main lobe direction (MLD).

study, the diameter of the half-cup is changed between D_C = 0.6 λ and D_C =1.4 λ, while its height is fixed at H_C = 0.5 λ. **Figure 12** shows the simulated radiation characteristics of the antenna for different values of D_C. As shown in this figure, increasing the diameter of the half-cup reflector increases the gain while decreases the HPBW and AR of the antenna. Moreover, variations of D_C also change the direction of the radiated beam. The figure shows that for small diameters of the half-cup reflector, e.g., D_C < 0.7 in **Figure 12c**, the polarization of the antenna is not circular because the AR is greater than 3dB. Furthermore, as shown in **Figure 12d**, for small values of D_C, the direction of the main beam is greater than 90°, i.e., the radiated beam is tilted toward the plasma half-cup. In contrast, further increasing the diameter of the half-

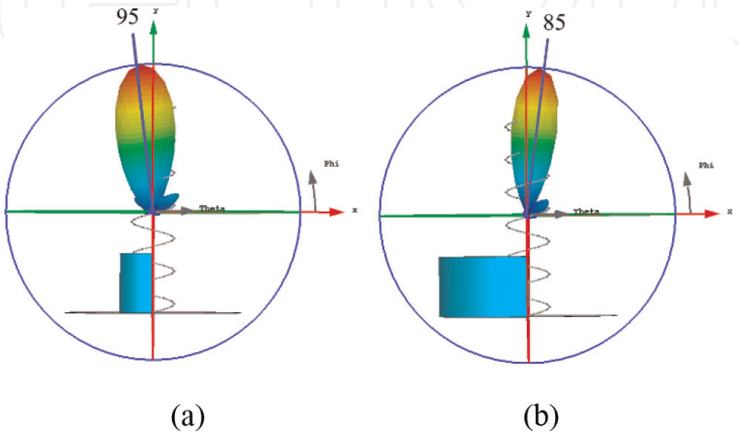

Figure 13.
Simulated radiation pattern of the plasma half-cupped-helical antenna at H_C = 0.5 λ when: (a) D_C = 0.6 λ, (b) D_C = 1.4 λ.

cup to the greater diameters than 0.7 λ, changes the direction of the main beam to the opposite side with respect to the half-cup, i.e., to angles smaller than 90 degrees. Based on these graphs, an optimum diameter of around 1.0 λ for the half-cup is also observed to achieve the maximum gain of 12.2 dBi with the circular polarization, while the beam is steered to 85°. In short, altering the diameter of the half-cup controls the direction of the main beam of the helical antenna, as shown in 3D radiation plots in **Figure 13** for two different diameters of the half-cup plasma reflector at H_C = 0.5 λ.

5. The effect of the height of the half-cup

Based on the results presented in the previous section, to compromise between a higher radiation gain and a lower AR for the antenna, a diameter of D_C = 1.0 λ is considered as the diameter of the half-cup in this section. By fixing D_C, the height of the half-cup plasma reflector (H_C) controls the physical shape of the half-cup. Thus, a parametric study is presented in this section based on the variation of H_C. The numerical results of the radiation characteristics of the antenna versus H_C, when it changes between H_C = 0 and H_C = 1.5 λ, are shown in **Figure 14**. The graphs clearly show that H_C changes all the radiation characteristics of the antenna. Specifically, the figure shows that for heights of smaller than 0.7 λ (H_C < 0.7 λ) the polarization of the antenna is circular (AR < 3 dB), and the maximum gain is achieved when $H_C \approx 0$, i.e. when there is no conductor reflector around the helix. The figures also show that increasing H_C from H_C = 0 to H_C = 0.7 λ decreases the radiation gain while steers the beam of the antenna from end-fire (i.e., θ = 90°) to θ = 84° in the opposite direction of the half-cup. Further increasing the H_C from 0.7 λ, increases the steering angle of the

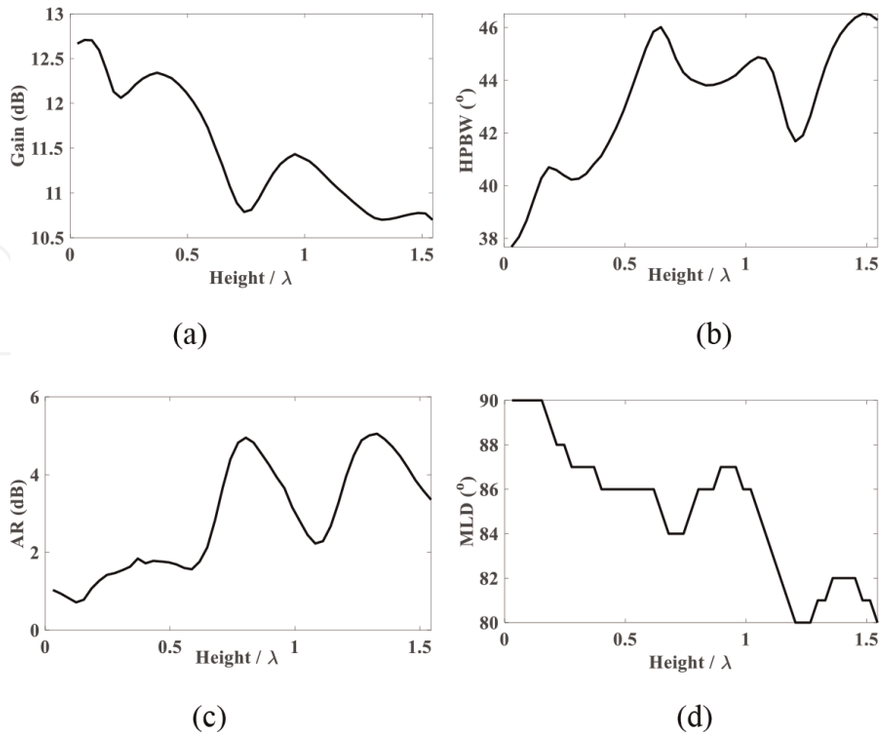

Figure 14.
Simulated radiation characteristics of the half-cupped-plasma antenna with a height of the cup at D_C = 1.0 λ: (a) gain, (b) HPBW, (c) AR, and (d) MLD.

DOI: http://dx.doi.org/10.5772/intechopen.108017

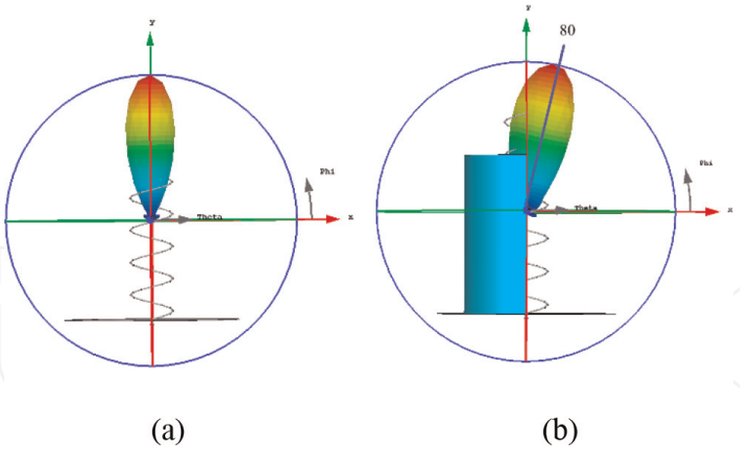

Figure 15.
Radiation of the half-cup plasma antenna with D_C = 1.0 λ when: (a) H_C = 0.0 λ, (b) H_C =1.25 λ.

main beam up to θ = 80°. However, the polarization of the antenna is not circular in this case. To have a better insight, 3-D radiation plots of the antenna for two special cases of H_C = 0.0 λ and H_C = 1.5 λ when D_C = 1.0 λ are shown in **Figure 15**.

In summary, from these graphs, it can be concluded that increasing the height of the half-cup steers the radiated beam of the helical antenna which is the target of this study. However, an appropriate selection of the height of the cup is required to achieve the maximum steering angle while maintaining the circular polarization using a half-cup plasma reflector around the helical antenna.

5.1 Summary

Dynamic beamwidth control and beam steering using plasma technology for the radiation beam of axial mode helical antennas is proposed. It has been shown that a circular array of plasma CFLs around the helical antenna controls electronically the direction and width of the radiated beam of the antenna. Fabrication of prototypes of the proposed structure and measurements of the radiation properties of various configurations of plasma reflectors confirmed the concept and computational results. The proposed antenna can be considered as a cost-effective solution for scanning and finding the target in certain applications related to space communications and radar systems.

5.2 Plasma helicone antenna

As previously mentioned in Section 3.1, an efficient technique to improve the radiation characteristics of a conventional axial mode helical antenna is shaping the ground conductor [40–44]. Some papers proposed a truncated conical reflector around an axial-mode helical antenna, known as a helicone antenna, in order to enhance its radiation gain, up to 5 dB, and also to minimize the side-lobe levels of helical antennas [42, 47, 48]. To compromise between the maximum radiation gain and minimum physical dimensions of the antenna, the optimal dimensions of the conical ground plane of the antenna have been presented in [42]. This antenna has applications in many communication systems where high radiation gain is desirable, including tracking and space communication systems.

Generally, a helicone antenna covers an area with a certain footprint. When the location of the target is known, a high-gain antenna will be preferred and this approach may be effective. However, when the location of the target is inaccurate, misalignment loss, especially in space applications, may be very high. In this case, if the beamwidth of the antenna in the ground station can be varied, even with less radiation gain, an alternate approach may be used. Using auto-tracking antenna pedestals is one method to address this issue. However, controlling the beamwidth of the ground station antenna is an alternative elegant method so that in normal conditions the antenna is adjusted to have its maximum gain, and when the target is lost, to find its accurate position its beamwidth is increased. For instance, to cover a relatively wide area, a conventional helical antenna with a relatively wide beamwidth can be used, and after receiving some information from the target, it can be reconfigured to have a narrower beamwidth (and as a result higher gain). The required reconfiguration from an antenna with a wider HPBW to an antenna with a higher gain is possible if the truncated conical ground of the antenna can be electrically switched ON and OFF or its dimension can be altered.

Although there are different techniques for controlling the beamwidth of a single antenna [49–52], it is critical that the selected technique minimizes the complexity of the hardware and software designs and as a result and reduces the costs associated with such an antenna. The aim of this study is to demonstrate a truncated conical plasma reflector around a conventional axial mode helical antenna as an efficient and relatively low-cost method to enhance the radiation gain and control HPBW of a helical antenna. It will be shown that there will be two radiation modes for the proposed antenna, namely, a narrow beam mode with higher radiation gain and a wide beam mode with lower radiation gain. To verify the performance of the proposed antenna, the simulation results of the designed antenna in terms of radiation gain and HPBW are presented. The results show that there are two different operating modes based on the state of the plasma. In the first mode, the plasma reflectors are switched OFF and the proposed structure acts as a conventional helical antenna, and in the second mode, the plasma reflectors are switched ON and the structure acts as a helical antenna with a truncated conical plasma reflector. As expected, in the second mode, the radiation gain is higher than the gain in the first mode. For the realization of the proposed structure, it is important to consider the feasibility, level of complexity, and the costs associated with the implementation. Thus, based on these considerations, different techniques for the implementation are analyzed and the best structure in terms of ease of fabrication is selected.

5.2.1 The basic structure of a helicone antenna

Figure 16 illustrates the structure of the helicone antenna which is composed of a conventional axial-mode helical antenna with a truncated conical ground. In this figure, *D, C, α, N,* and *L* are, respectively, the diameter, the circumference, the pitch angle, the number of turns, and the length of the helical section of the antenna. For the truncated conical section, D_1, D_2, β, and H are, respectively, the inner diameter, the outer diameter, the angle, and the height. The operating frequency of the antenna is 1280 MHz. At this frequency, the dimensions of the helical section of the antenna are $D = 8.4$ cm, $C = 1.12\,\lambda$, $\alpha = 11.35^{\circ}$, $N = 5$, and $L \approx 26.49$ cm. Considering a circular ground plane with the radius of $D_g = 1.5\,D$ for the designed helical antenna, which is used as a reference in this study, the simulated radiation gain and beamwidth

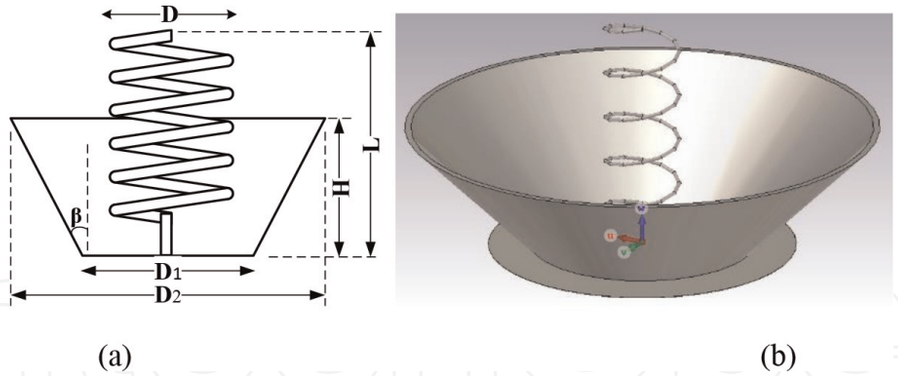

Figure 16.
(a) The structure of a conventional helicone antenna, (b) an illustration of the antenna.

are, respectively, G = 12.6 dBi and HPBW = 40.6° while the direction of the main beam of the helix is in the end-fire direction at θ= 90°.

Based on the study presented in [42], the optimum dimensions of the truncated conical ground section for the maximum gain are D_1 = 1.1 λ, H = 0.6 λ, and β =45°, which for the operating frequency of 1280 MHz, D_1 = 25.78 cm, and H = 14.06 cm. For the optimized helicone antenna, the simulated radiation gain and beamwidth are, respectively, G = 15 dBi and HPBW = 31.7° in the end-fire direction, while the polarization of the antenna is still circular. So, around 19% enhancement in the radiation gain of the optimized helicone antenna with respect to a circular ground plane helical antenna is observed while, as expected, the HPBW of the antenna has proportionally decreased.

5.2.2 A helicone antenna using plasma conical ground

In this section, a helicone antenna using a truncated conical ground of the plasma material is analyzed numerically. Here, the plasma and collision frequencies are, respectively, ω_p = 14 $\times 10^{10}$ rad/s and ν = 400 MHz, the height of the cone is 0.6 λ and its angle is 45°. The simulation results show a gain of G = 15.3 dBi and beamwidth of HPBW = 31.2° for the antenna, which proves that the performance of the plasma conical ground is similar to the performance of the metallic conical ground. Moreover, it is clear that by switching OFF the plasma section, the radiation gain and beamwidth of the antenna, just like a single helical antenna, are, respectively, G = 12.6 dBi and HPBW = 40.6°, as shown in **Figure 17**. So, the helical antenna with plasma conical ground is capable of switching between two different radiation patterns, by switching the plasma conical ground ON and OFF. When the plasma conical ground is switched

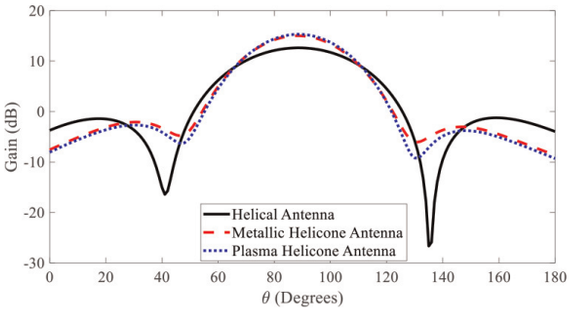

Figure 17.
The simulated radiation gain of the helicone antenna using a plasma conical reflector.

ON, a helicone antenna is achieved which benefits from a higher radiation gain (or narrower beamwidth) and when the plasma reflector is switched OFF a helical antenna is achieved with lower radiation gain (or wider beamwidth).

5.2.3 The implementation of the plasma helicone antenna

Numerical results presented in the previous section show that a truncated conical plasma reflector provides a switchable beamwidth (or gain) for the helical antenna. In practice, the realization of the homogenous conical section by plasma material is not straightforward. So, the aim of this section is to analyze different conical structures based on the commercial fluorescent lamps for the realization of the plasma conical reflector. To this end, different structures are analyzed and their performances are evaluated.

5.2.4 Plasma helicone antenna based on the U-shaped compact fluorescent lamps

As the first method for the realization of the plasma helicone antenna, as shown in **Figure 18**, a sufficiently dense array of U-shaped CFLs are arranged in a conical structure. The dimensions of a U-shaped CFL has been shown in **Figure 6b**. The number of CFLs in the structure is selected based on the circumference of the bottom face of the cone so that a dense array of CFLs covers this face. The length of each CFL is 18 cm from the circular ground and the diameter of each CFL column is 14.7 mm, while a 1.6 mm space gap is between the columns. So, to form the truncated conical reflector, 19 CFLs are arranged at the bottom face of the cone. The angle between the ground plane and each CFL is 45°. Note that the packaging of the commercial off-the-shelf CFLs is such that small space gaps between adjacent elements are inevitable. It is clearly observed in the figure that the distance between the CFLs in the larger diameter of the cone (i.e. D_2) is not possible to be ignored. So, discrepancies between the performance of the conical-shaped homogenous plasma reflector and the conical reflector using U-shaped CFLs are expected. The simulated radiation gain and beamwidth of the plasma helicone antenna with based on the proposed structure are G = 12.8 dBi and HPBW = 37.8° compared to G =12.6 dBi and HPBW = 30.6° for the helical reference antenna (without the conical ground). This structure shows less than 2% improvement in the radiation gain of the antenna, while the total power consumption of the antenna is 342 W.

5.2.5 Plasma helicone antenna based on the fluorescent tubes

In this case, 45 commercial conventional fluorescent lamps are arranged in a conical shape to form the reflector, as shown in **Figure 19**. The diameter and length of

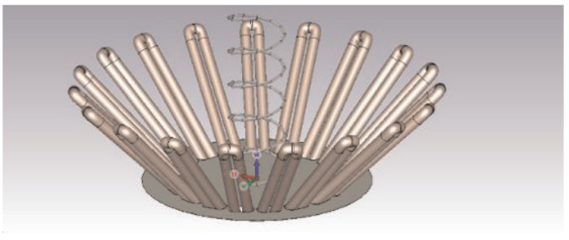

Figure 18.
The structure of the helicone antenna using U-Shaped CFLs.

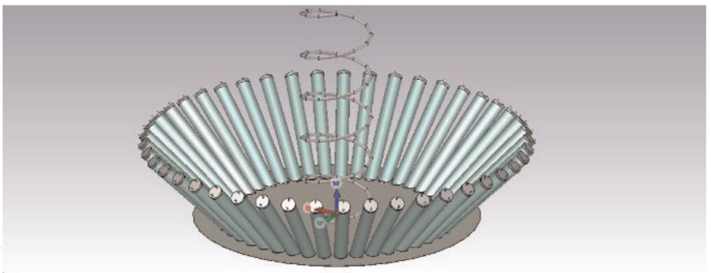

Figure 19.
The structure of the helicone antenna using commercial fluorescent lamps.

the fluorescent lamps are 1.5 cm and 18 cm, respectively. The plasma and collision frequencies are, respectively, $\omega_p = 14 \times 10^{10}$ rad/s and $\nu = 400$ MHz for each lamp. Since the power consumption of each lamp is 6 W, the total power consumption of this structure is 270 W. The simulated radiation gain and HPBW of the helicone antenna based on this structure are, respectively, G = 13.1 dBi and HPBW = 37° when all the lamps are excited. This shows a 3% improvement in the radiation gain with respect to the reference helical antenna. It seems that this structure is also inefficient because the distance between the plasma elements in the upper section of the conical reflector is large.

5.2.6 Plasma helicone antenna based on the combination of U-shaped CFLs and fluorescent lamps

In order to improve the radiation gain of the plasma helicone antenna, a new version of the truncated conical reflector is proposed here based on the combination of the U-shaped CFLs and cylindrical fluorescent lamps. In this structure, 19 U-shaped CFLs are arranged in the structure shown in **Figure 18**, while 19 fluorescent lamps are also inserted between them from the upper side of the cone, as shown in **Figure 20**. The holder of the fluorescent tubes is made from Teflon. The simulated radiation gain and beamwidth of this structure are, respectively, G = 14.7 dBi and HPBW = 30°, which around 17% enhancement in the gain is observed with respect to the reference helical antenna. The power consumption of this structure is around 459 W.

5.2.7 Plasma helicone antenna based on a spiral plasma tube

As another alternative for the implementation of the conical ground in the helicone antenna, the effects of a spiral plasma lamp are also investigated. A view of the

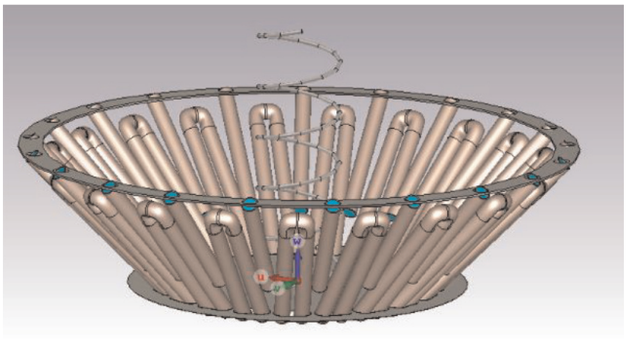

Figure 20.
3-D view of a helicone antenna based on the combination of fluorescent lamps and U-shaped CFLs.

proposed structure is shown in **Figure 21**. The diameter and thickness of the spiral plasma tube are, respectively, 1 cm 0.1 cm while the tube material is Pyrex. To form the conical plasma section, around 17 turns of the plasma tube are wrapped in this study. The plasma and collision frequencies are around ω_p = 14 $\times 10^{10}$ rad/s and ν = 400 MHz in the column. The simulated radiation gain and beamwidth of this antenna are around G = 14.6 dBi and HPBW = 33.9°, respectively. Around 16% enhancement with respect to the reference helical antenna is observed in the radiation gain using this structure which is similar to the enhancement of the radiation gain in the previous case in which a combination of fluorescent lamps and U-shaped CFLs are used for the implementation of the conical section. A comparison between the simulated gain of the helical antenna using proposed plasma reflectors in the two last cases with the gain of the reference helical and helicone antennas is shown in **Figure 22**.

5.2.8 Reconfigurable slotted cylindrical waveguide and coaxial array plasma antenna

Slotted waveguide antennas have been studied in the literature for many years [53–59]. A number of papers [60–64] have proposed plasma-filled waveguides for mode modification or as protection against high-power electromagnetic waves. In this study, the waveguide is partially filled with plasma. In this section, we propose a reconfigurable cylindrical slotted waveguide antenna coupled to a plasma tube, and study the radiation pattern, gain, S-parameters, and we present simulation and experimental results related to efficiency and performance. This antenna system offers him two modes of operation depending on the plasma conditions. 1) the waveguide mode, which is active when the plasma is off, and 2) the coaxial mode, when the plasma is on. Performance of the reconfigurable system is observed in terms of reflection coefficient, maximum realizable gain, radiation pattern, and overall efficiency. Slotted waveguide antennas have been studied in the literature for many years

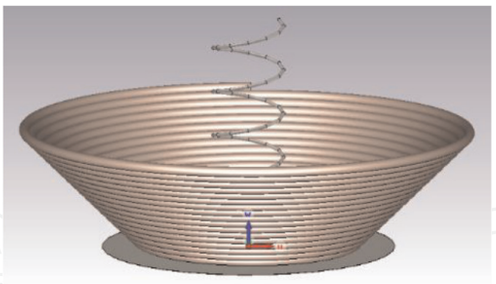

Figure 21.
The structure of the helicone antenna using conical spiral plasma lighting tubes.

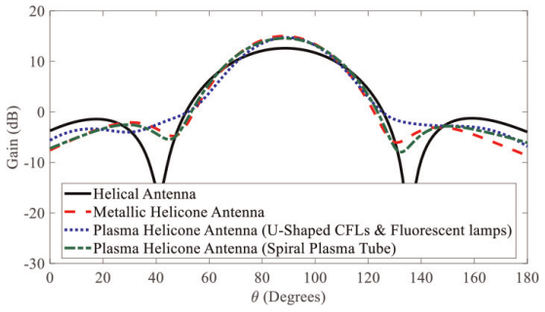

Figure 22.
The simulated radiation gain of the helicone antenna for different cases.

[53–59]. A number of papers [60–64] have proposed plasma-filled waveguides for mode modification or as protection against high-power electromagnetic waves. In this study, the waveguide is partially filled with plasma. In this section, we propose a reconfigurable cylindrical slotted waveguide antenna coupled to a plasma tube, and study the radiation pattern, gain, S-parameters, and We present simulation and experimental results related to efficiency and performance. This antenna system offers her two modes of operation depending on the plasma conditions. 1) the waveguide mode, which is active when the plasma is off, and 2) the coaxial mode, when the plasma is on. Performance of the reconfigurable system is observed in terms of reflection coefficient, maximum realizable gain, radiation pattern, and overall efficiency.

5.3 Modeling and simulation

The shape of the waveguide is shown in **Figure 23**. The diameter and length of the metal tube are 70 mm and 620 mm, respectively. A plasma tube, which is a commercially available fluorescent lamp, is inserted into the metal tube (see **Figure 24a** and **b**). The height and diameter of the lamp are 590 mm and 26 mm, respectively. The feed system consists of a metal ring surrounding both ends of the lamp and a coaxial cable (see **Figure 24a**) attached to this metal ring to provide the RF signal. The realized prototype is shown in **Figure 24b**. In this study, CST Microwave Studio is used for simulation. The gas-containing tube consists of glossy glass with εr = 4.82, tan δ = 0.005 and a thickness of 0.5 mm. The plasma follows the Drude model [65, 66]

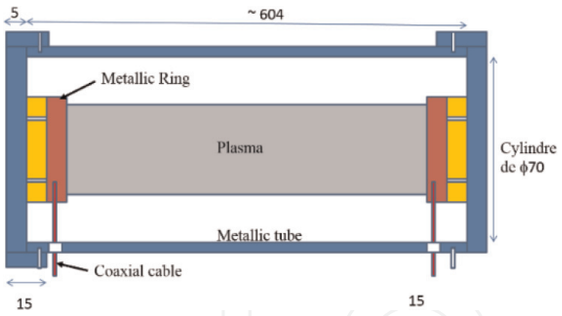

Figure 23.
Antenna shape.

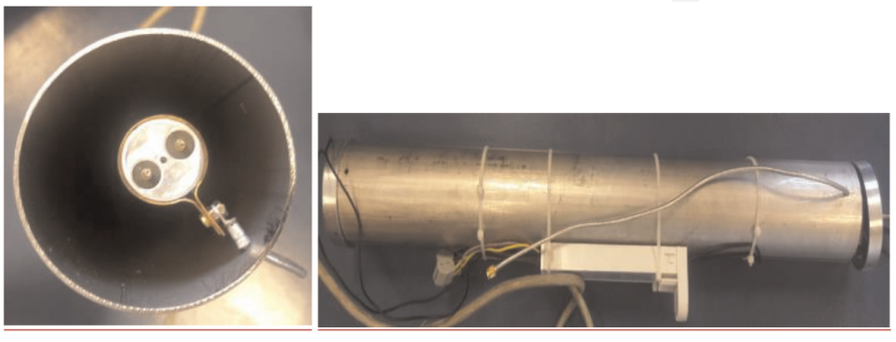

Figure 24.
Realized models. (a) Feeding lamp. (b) Realized waveguide.

defined by two parameters: plasma angular frequency ωp = 43.9823×109 rad/s and electron neutral collision frequency ν = 900 MHz.

5.4 Results and discussion

5.4.1 Plasma waveguide antenna

First, we investigate the S-parameters of the antenna and examine the behavior of the metal tube depending on the plasma state. **Figure 25** shows simulated S11 and S21 of the proposed structure for both plasma off and plasma on cases. Note that when the plasma is turned off, we expect a conventional waveguide with a cutoff frequency of about 2.5 GHz, as shown in **Figure 25a**. However, when the plasma is on, the coaxial conductor appears with stronger absorption around 4 GHz, as shown in **Figure 25b**.

In order to validate the simulation results, S21 measurements were carried out in cases of plasma activation and deactivation, as shown in **Figure** 26. Simulations and measurements agree, but the observed loss is more significant. Plasma OFF curves indicate low-frequency lamps, possibly due to prototype and delivery system manufacturing.

5.4.2 Slotted waveguide antenna

Now, to use the metal tube as an antenna, make 12 small slits (ls = 40mm, ws = 5mm) in the surface of the tube, as shown in **Figure** 27. The distance between the slots

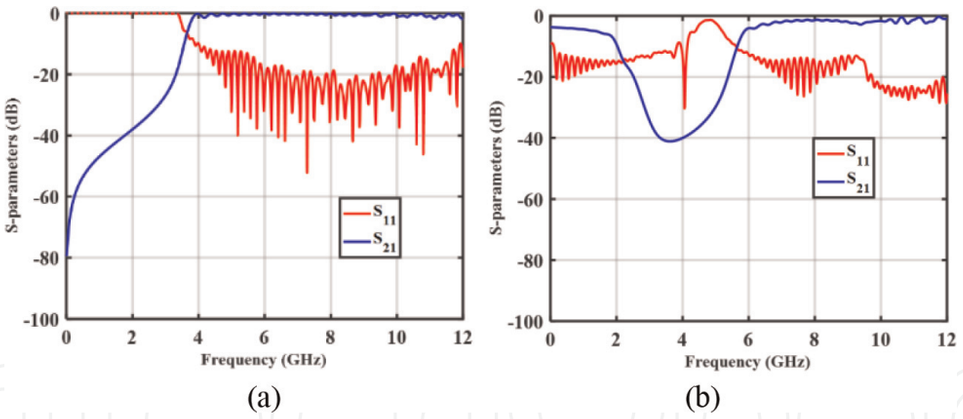

Figure 25.
Simulated S11 and S21 magnitude. (a) Plasma is OFF. (b) Plasma is ON.

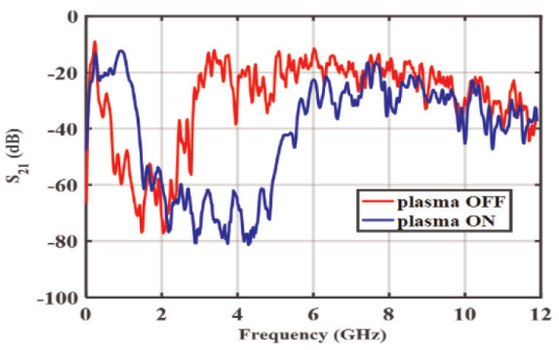

Figure 26.
Measured S21 magnitude when the plasma is OFF and ON.

Figure 27.
Slotted waveguide geometry, small slot for 4 GHz antenna (ls = 40 mm, ws = 5 mm) and large slot for 1 GHz antenna (ls = 150 mm, ws = 5 mm).

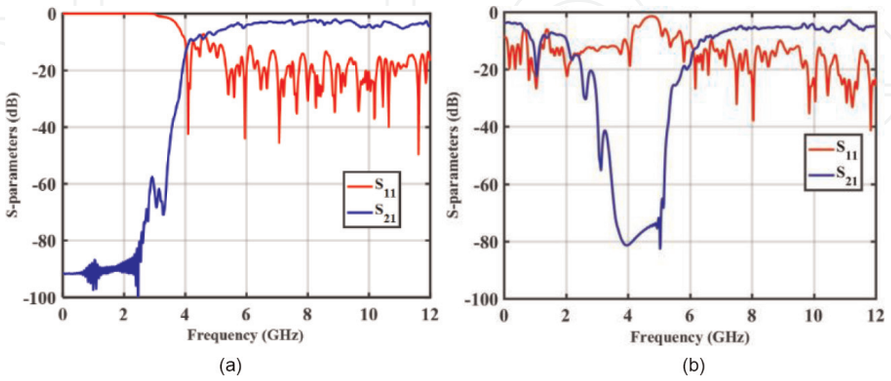

Figure 28.
Simulated sizes of S11 and S21 for slot antennas. (a) Plasma is off. (b) Plasma is on.

is λ/2 to 4 GHz (40 mm), so the antenna radiates up to 4 GHz with the plasma turned off. It also has four large slots (ls = 150 mm, ws = 5 mm) and a slot spacing of λ/2 at 1 GHz (150 mm). The antenna operates at 1 GHz when the plasma is on.

Figure 28 shows the S11 and S21 simulations of the slotted antenna both when the plasma is off (**Figure 28a**) and on (**Figure 28b**). The match around 4GHz is -40dB and the S21 is -10dB. This means that most of the power is radiated resulting in good gain and efficiency. By turning on the plasma, the 1 GHz match due to the waveguide to coaxial line conversion is -20 dB and S21 is about -20 dB. In this case, a 4-element array provides good gain and efficiency.

A radiation pattern is shown in **Figure 2** to demonstrate the reconfigurable capability of this antenna system. **Figure 29a** and **29b** show simulated E-plane radiation patterns for 4 GHz frequency when plasma is off and 1 GHz frequency when plasma is on, respectively. In the two simulation results, each radiation pattern is normalized to

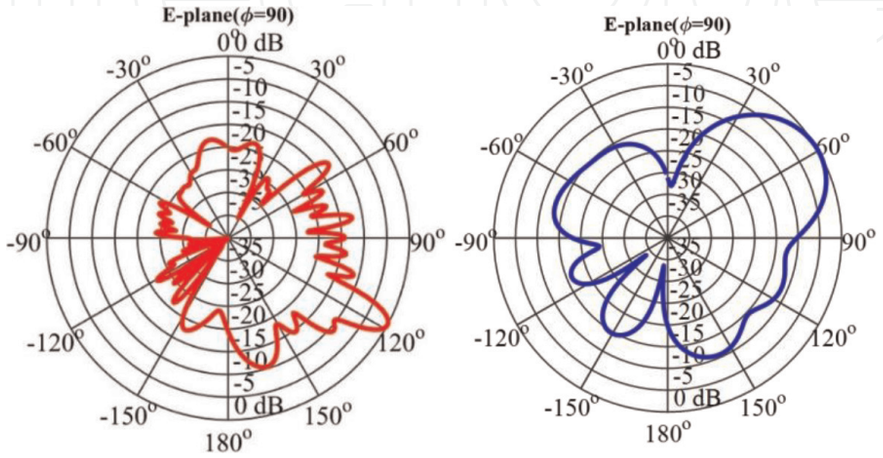

Figure 29.
Normalized H-plane radiation pattern. (a) 4 GHz with the plasma turned off. (b) 1 GHz with plasma ON.

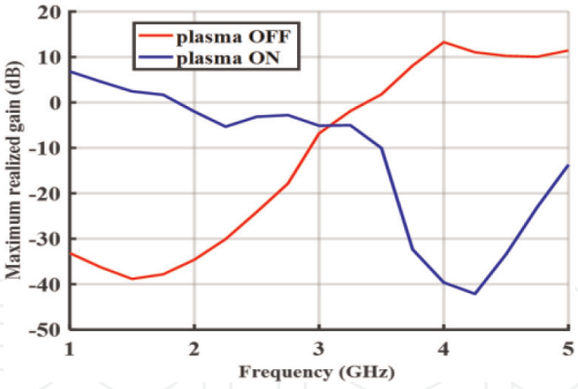

Figure 30.
Gain of the antenna in plasma OFF and ON cases.

its electric field maximum. The -3 dB simulation bandwidths are 8.1° to 4 GHz and 34.1° to 1 GHz. The antenna is tilted between two frequencies, 120° to 4 GHz and 60° to 1 GHz. Sidelobe level (SLL) is close to -10dB regardless of configuration.

Figure 30 shows the maximum simulation gain achieved. For plasma shutdown, the gain is maximum at 4 GHz, 13.27 dBi. In the case of ON, the gain is maximal at 1 GHz and is equivalent to 6.82 dBi. As far as gain is concerned, there is a 40 dB to 1 GHz difference between plasma OFF and plasma ON. The difference of 52 dB to 4 GHz between switched-off plasma and activated plasma. Normally, the antenna is not expected to operate at 1 GHz because the cut-off frequency is greater than 1 GHz. But once the lamp is switched on, the waveguide becomes a coaxial line from which to obtain radiation and gain at 1 GHz. Gain allows evaluation of antenna efficiency. Total efficiency is 83.4% to 4 GHz (extinguished plasma) and 68.2% to 1 GHz (activated plasma).

6. Conclusion

In this chapter, several approaches for the dynamic control of the beamwidth and radiation gain of circular polarized helical antennas based on plasma reflectors have been presented. The concept and design principles were discussed and confirmed through complete full-wave simulations. Various achievements of the plasma reflector, using U-shaped CFLs, commercial fluorescent tubes and conical spiral plasma tubes have been explored. From the upper and lower side of the cone, the most effective solution is to replace the metallic truncated conical reflector by a combination of U-shaped CFLs and commercial fluorescent tubes.

In all cases, we look at the practicalities and costs of implementation.

In the last section, a reconfigurable slot antenna using a plasma tube inside a metal waveguide was presented. The antenna exhibits reconfigurable radiation patterns at 4 GHz and 1 GHz, depending on the plasma conditions. The main advantage of this antenna with the plasma on is that it can radiate at 1 GHz while the gain drops off sharply at 4 GHz frequency.

DOI: http://dx.doi.org/10.5772/intechopen.108017

Author details

Fatemeh Sadeghikia[1*], Ali Karami Horestani[1] and Mohamed Himdi[2]

1 Wireless Telecommunication Group, ARI, Ministry of Science, Research and Technology, Tehran, Iran

2 IETR, University of Rennes 1, Rennes, France

*Address all correspondence to: sadeghi_kia@ari.ac.ir

References

[1] Sadeghikia F, Dorbin MR, Horestani AK, Noghani MT, Ja'afar H. Tunable inverted F antenna using plasma technologies. IEEE Antennas and Wireless Propagation Letters. 2019; **18**(4):702-706

[2] Ja'afar H, Ali MTB, Dagang ANB, Zali HM, Halili NA. A reconfigurable monopole antenna with fluorescent tubes using plasma windowing concepts for 4.9-GHz application. IEEE Transaction on Plasma Science. 2015;**43**(3):815-820

[3] Alexeff I, Anderson T, Parameswaran S, Pradeep EP, Hulloli J, Hulloli P. Experimental and theoretical results with plasma antennas. IEEE Transactions on Plasma Science. 2006; **34**(2):166-172

[4] Jusoh MT, Lafond O, Colombel F, Himdi M. Performance and radiation patterns of a reconfigurable plasma corner-reflector antenna. IEEE Antennas and Wireless Propagation Letters. 2013; **12**:1137-1140

[5] Yuan X, Li Z, Rodrigo D, Mopidevi H, Kaynar O, Jofre L, et al. A parasitic layer-based reconfigurable antenna design by multi-objective optimization. IEEE Transactions on Antennas and Propagation. 2012;**60**(6):2690-2701

[6] Plapous C, Cheng J, Taillefer E, Hirata A, Ohira T. Reactance domain music algorithm for electronically steerable parasitic array radiator. IEEE Transactions on Antennas and Propagation. 2004;**52**(12):3257-3264

[7] Fourikis N. Phased Array-Based Systems and Applications. Newyork: Wiley; 1997

[8] Jusoh MT, Lafond O, Colombel F, Himdi M. Performance of a reconfigurable reflector antenna with scanning capability using low-cost plasma elements. Microwave and Optical Technology Letters. 2013;**55**(12): 2869-2874

[9] Barro OA, Lafond O, Himdi H. Reconfigurable antennas radiations using plasma Faraday cage. In: 2015 international Conference on Electromagnetics in Advanced Applications (ICEAA). Turin, Italy: ICEAA; 07-11 Sep 2015. pp. 545-548

[10] Sadeghikia F, Noghani MT, Simard M. Experimental study on the surface wave driven plasma antenna. AEU International Journal of Electronic Communication. 2016;**70**:652-656

[11] Sadeghikia F, Dorbin MR, Horestani AK, Noghani MT, Ja'afar H. Multi-beam frequency tunable antenna based on plasma-nested helix. In: 2019 13th European conference on antennas and propagation (EuCAP). Krakow, Poland: EuCAP; 31 Mar - 05 Apr 2019. pp. 1-3

[12] Dorbin MR, Mohassel R, Sadeghikia F, Binti Ja'afar H. Analytical estimation of the efficiency of surface-wave-excited plasma monopole antennas. IEEE Transactions on Antennas and Propagation. 2022;**70**(4): 3040-3045

[13] Dorbin MR, Rashed Mohassel JA, Sadeghikia F, Ja'afar HB. Analytical Estimation of the Efficiency of Surface-Wave-Excited Plasma Monopole Antennas. In: IEEE Transactions on Antennas and Propagation. Vol. 70. No. 4. Apr 2022. pp. 3040-33045

[14] Sadeghikia F, Doorbin MR, Jaafar H, Horestani AK, Noghani MT. An overview on the implementation of

surface wave driven plasma antennas. In: IEEE Symposium on Wireless Technology & Applications (ISWTA). Malaysia; 2021. pp. 53-57

[15] Sadeghikia F, Horestani AK, Dorbin MR, Noghani MT, Ja'afar H. A new feed network for the communication signal and excitation of surface-wave-driven plasma antennas. In: 2020 14th European Conference on Antennas and Propagation (EuCAP). Copenhagen, Denmark: EuCAP; 15-20 Mar 2020. pp. 1-4

[16] Noghani MT, Horestani AK, Sadeghikia F, Dorbin MR. Theoretical modeling of resonant wavelength in 3-layered plasma antennas. Waves in Random and Complex Media. 2021; **31**(6):1587-1596

[17] Sadeghikia F, Hodjat-Kashani F, Rashed-Mohassel J, Ghayoomeh-Bozorgi J. The effects of the tube characteristics on the performance of a plasma monopole antenna. In: Proc. 32nd PIERS Conf. in Moscow. Russia; 2012. pp. 1208-1211

[18] Sadeghi-Kia F. Analysis of plasma monopole antenna using numerical method and an equivalent circuit. IEEE Antennas and Wireless Propagation Letters. 2017;**16**:1711-1714

[19] Sadeghikia F, Hodjat-Kashani F. A two element plasma antenna array. Engineering, Technology & Applied Science Research. 2013;**3**(5):516-521

[20] Sadeghikia F, Hodjat-Kashani F, Rashed-Mohassel J, Ghayoomeh-Bozorgi J. Characterization of a surface wave driven plasma monopole antenna. Journal of Electromagnetic Waves and Applications. 2012;**26**(2/3):239-250

[21] Sadeghikia F, Hodjat-Kashani F, Rashed-Mohassel J, Ghayoomeh-Bozorgi J. Characteristics of plasma antennas under radial and axial density variations. In: PIERS Conference in Moscow. Russia; 2012. pp. 1212-1215

[22] Sadeghikia F, Hodjat-Kashani F, Rashed-Mohassel J, Lotfi AA, Ghayoomeh-Bozorgi J. A Yagi-UDA plasma monopole array. Journal of Electromagnetic Waves and Application. 2012;**26**:885-894

[23] Sadeghikia F, Horestani AK, Noghani MT, Dorbin MR, Mahdikia H, Ja'afar H. A study on the effect of the radius of a cylindrical plasma antenna on its radiation efficiency. International Journal of Engineering and Technology. 2018;**7**:204-206

[24] Sadeghikiya F, Hojatkashani F, Rashed Mohasel J, Ghiyome Bozorgi SJ. Space application of a linear array of plasma antenna. Journal of Space Science and Technology. 2012;**5**(3):59-66

[25] Sadeghi-Kia F, Hodjat-Kashani F, Rashed-Mohassel J. Analysis of tapered column plasma using full wave simulator. In: Loughborough Antennas & Propagation Conference (LAPC). Loughborough, UK; 2009

[26] Sadeghikia F, Hodjat-Kashani F, Rashed-Mohassel J. An investigation on surface wave driven plasma monopole antenna. Journal of Iranian Association of Electrical and Electronics Engineers. 2013;**10**(1):7-16

[27] Noghani MT, Sadeghikia F, Dorbin MR, Horestan AK. Analysis of surface waves in a 3-layered cylindrical plasma antenna. In: 27th Iranian Conference on Electrical Engineering (ICEE). Iran; 2019. pp. 1425-1428

[28] Valipour M, Sadeghikia F, Karami-Horestani A, Ja'afar H. The effect of non-uniform conductivity on radiation

characteristics of a monopole plasma antenna. In: 13th European Conference on Antennas and Propagation (EUCAP). Krakow, Poland; 2019

[29] Horestani AK, Noghani MT, Sadeghikia F, Dorbin MR, Valipour M, Martín F. Reconfigurable and frequency tunable inverted F antenna based on plasma technology. In: International Conference on Electromagnetics in Advanced Applications (ICEAA). Granada, Spain; 2019. pp. 1175-1177

[30] Ja'afar H, Abdullah R, Redzwan FNM, Sadeghikia F. Analysis of cylindrical monopole plasma antenna design. In: International Symposium on Antennas and Propagation (ISAP). Busan, Korea (South); 2018. pp. 1-2

[31] Sadeghikia F, Noghani MT, Dorbin MR, Seyyedi J, Jabbari A. A study on the physical characteristics and development of plasma reflectors. Journal of Radar. 2021;**7**(1):35-44

[32] Sadeghikia F. Plasma antenna technology in space missions. Journal of Space Science and Technology. 2017; **10**(1):27-34

[33] Moisan M, Nowakowska H. Contribution of surface-wave (SW) sustained plasma columns to the modeling of RF and microwave discharges with new insight into some of their features. A survey of other types of SW discharges. Plasma Sources Science and Technology. 2018;**27**(7)

[34] Manheimer W. Plasma reflectors for electronic beam steering in radar systems. IEEE Transactions on Plasma Science. 1993;**19**(6):1228-1234

[35] Anderson T. Fundamental plasma antenna theory. In: Plasma Antennas. Norwood, MA, USA: Artech House; 2011

[36] Ha A, Chae MH, Kim K. Beamwidth control of an impulse radiating antenna using a liquid metal reflector. IEEE Antennas and Wireless Propagation Letters. 2019;**18**(4):571-575

[37] Chatterjee A, Parui SK. Beamwidth Control of Omnidirectional antenna using conformal frequency selective surface of different curvatures. IEEE Transactions on Antennas and Propagation. 2018;**66**(6):3225-3230

[38] Debogović T, Perruisseau-Carrier J. Array-fed partially reflective surface antenna with independent scanning and beamwidth dynamic control. IEEE Transactions on Antennas and Propagation. 2014;**62**(1):446-449

[39] Towfiq A, Bahceci I, Blanch SA, Romeu J, Jofre L, Cetiner BA. A reconfigurable antenna with beam steering and beamwidth variability for wireless communications. IEEE Transactions on Antennas and Propagation. 2018;**66**(10):5052-5063

[40] Sadeghikia F, Valipour M, Noghani MT, Ja'afar H, Horestani AK. 3D beam steering end-fire helical antenna with beamwidth control using plasma reflectors. IEEE Transactions on Antennas and Propagation. 2021;**69**(5): 2507-2512

[41] Djordjevic AR, Zajic AG, Ilic MM. Enhancing the gain of helical antennas by shaping the ground conductor. IEEE Antennas and Wireless Propagation Letters. 2006;**5**:138-140

[42] Sadeghikia F, Horestani AK. Design guidelines for helicone antennas with improved gain. Microwave Optics Technology Letters. 2019;**61**(4):1016-1021

[43] Sadeghkia F, Mahmoodi M, Hashemi-Mehneh H, Ghayoomeh J.

Helical antenna over different ground planes. In: 8th European Conference on Antennas and Propagation (EuCAP). The Hague, Netherlands: EuCAP; 06-11 Apr 2014. pp. 2185-2188

[44] Valipour M, Sadeghikia F, Karami-Horestani A, Himdi M. Beamwidth control of a helical antenna using truncated conical plasma reflectors. In: 14th European Conference on Antennas and Propagation (EuCAP). Denmark; 2020

[45] Sadeghikia F, Mahdikia H, Dorbin MR, Noghani MT, Horestani AK, Jaafar H. A study on the effect of gas pressure and excitation frequency of a cylindrical plasma antenna on its radiation efficiency. In: 13th European Conference on Antennas and Propagation (EuCAP). Poland; 2019

[46] Sadeghikia F, Valipour M, Horestani AK, Himdi M, Anderson T. Beam-steerable helical antenna using plasma reflectors. In: 16th European Conference on Antennas and Propagation (EuCAP). Madrid, Spain; 2022

[47] Olcan DI, Zajic AR, Ilic MM, Djordjevic AR. On the optimal dimensions of helical antenna with truncated cone reflector. In: 1st European Conference on Antennas and Propagation. Nice, France; 2006

[48] King H, Wong J. Characteristics of 1 to 8 wavelength uniform helical antennas. IEEE Transactions on Antennas and Propagation. 1980;**28**(2):291-296

[49] Weily AR, Bird TS, Guo YJ. A reconfigurable high-gain partially reflecting surface antenna. IEEE Transactions on Antennas and Propagation. 2008;**56**(11):3382-3390

[50] Deng WQ, Yang XS, Shen CS, Zhao J, Wang BZ. A dual-polarized pattern reconfigurable Yagi patch antenna for microbase stations. IEEE Transactions on Antennas and Propagation. 2017;**65**(10):5095-5102

[51] Debogovic T, Bartoli J, Perruisseau-Carrier J. Array-fed partially reflective surface antenna with dynamic beamwidth control and beamsteering. In: 2012 6th European Conference on Antennas and Propagation (EUCAP). Prague, Czech Republic: EUCAP; 26-30 Mar 2012. pp. 3599-3603

[52] Towfiq MA, Bahceci I, Blanch S, Romeu J, Jofre L, Cetiner BA. A reconfigurable antenna with beam rteering and beamwidth variability for wireless communications. IEEE Transactions on Antennas and Propagation. 2018;**66**(10):5052-5063

[53] Wang W, Jin J, Liang X-L, Zhang Z-H. Broadband dual polarized waveguide slotted antenna array. In: 2006 IEEE Antennas and Propagation Society International Symposium. Albuquerque, NM: IEEE; 09-14 Jul 2006. pp. 2237-2240

[54] Park S, Tsunemitsu Y, Hirokawa J, Ando M. Center feed single layer slotted waveguide array. IEEE Transactions on Antennas and Propagation. 2006;**54**(5): 1474-1480

[55] Harmouch A, Haddad HSA. Cylindrical omnidirectional slotted waveguide antenna with optimized directional characteristics. In: 2013 13th Mediterranean Microwave Symposium (MMS). Saida, Lebanon: MMS; 02- 05 Sep 2013. pp. 1-4

[56] Li T, Meng H, Dou W. Design and implementation of dual- frequency dual-polarization slotted waveguide antenna array for Ka- band application. IEEE Antennas and Wireless Propagation Letters. 2014;**13**:1317-1320

[57] Mondal P, Chakrabarty A. Slotted waveguide antenna with two radiation nulls. IEEE Transactions on Antennas and Propagation. 2008;**56**(9): 3045-3049

[58] Lu X, Wang X, Lu W. A low-profile parallel plate waveguide slot antenna array for dual-polarization application. In: 2017 11th European Conference on Antennas and Propagation (EUCAP). Paris, France: EUCAP; 19-24 Mar 2017. pp. 970-972

[59] Fan G-X, Jin J-M. Scattering from a cylindrically conformal slotted waveguide array antenna. IEEE Transactions on Antennas and Propagation. 1997;**45**(7):1150-1159

[60] Tomar K. Sanjay and Malik, Hitendra, "Density modification by two superposing TE10 modes in a plasma filled rectangular waveguide". Physics of Plasmas

[61] Silvio H, Jankovic G. Scanning Leaky-wave Antenna based on a Waveguide filled with Plasma-like ENG Metamaterial. In: 2006 - MELECON, IEEE Mediterranean Electrotechnical Conference. Malaga, Spain: IEEE; 2006. pp. 280-283

[62] Hirani RR, Pathak SK, Shah SN, Sharma DK. Dispersion characteristics of dielectric tube waveguide loaded with plasma for leaky wave antenna application. AEU – International Journal of Electronics and Communications. 2018;**83**:123-130

[63] Anderson T, Alexeff I. Ân´ Reconfigurable electromagnetic plasma waveguide used as a phase shifter and a horn antenna US6812895B2. 2004

[64] Esteban J, Camacho-Penalosa C, Page JE, Martin-Guerrero TM, Marquez-Segura E. Simulation of negative permittivity and negative permeability by means of evanescent waveguide Modes-theory and ex- periment. IEEE Transactions on Microwave Theory and Techniques. 2005;**53**(4):1506-1514

[65] Barro OA, Himdi M, Lafond O. Reconfigurable patch antenna radiations using plasma faraday shield effect. IEEE Antennas and Wireless Propagation Letters. 2016;**15**:726-729

[66] Barro OA, Himdi M, Lafond O. Reconfigurable radiating antenna array using plasma tubes. IEEE Antennas and Wireless Propagation Letters. 2016;**15**: 1321-1324